Title

Feasibility evaluation of diffusion-weighted imaging using an integrated MRI-radiotherapy system for response assessment to neoadjuvant therapy in rectal cancer.

Journal

The British journal of radiology, 90(1071)

ISSN

0007-1285

Authors

Shaverdian, Narek
Yang, Yingli
Hu, Peng
et al.

Publication Date

2017-03-01

DOI

10.1259/bjr.20160739

Peer reviewed

BJR

Received: 7 September 2016 | Revised: 4 January 2017 | Accepted: 9 January 2017

https://doi.org/10.1259/bjr.20160739

Cite this article as:
Shaverdian N, Yang Y, Hu P, Hart S, Sheng K, Lamb J, et al. Feasibility evaluation of diffusion-weighted imaging using an integrated MRI-radiotherapy system for response assessment to neoadjuvant therapy in rectal cancer. *Br J Radiol* 2017; **90**: 20160739.

SHORT COMMUNICATION

Feasibility evaluation of diffusion-weighted imaging using an integrated MRI-radiotherapy system for response assessment to neoadjuvant therapy in rectal cancer

[1]NAREK SHAVERDIAN, MD, [1]YINGLI YANG, PhD, [2]PENG HU, PhD, [3]STEVEN HART, MD, [1]KE SHENG, PhD, [1]JAMES LAMB, PhD, [1]MINSONG CAO, PhD, [1]NZHDE AGAZARYAN, PhD, [1]DAVID THOMAS, PhD, [1]MICHAEL STEINBERG, MD, [1]DANIEL A LOW, PhD and [1]PERCY LEE, MD

[1]Department of Radiation Oncology, University of California, Los Angeles, CA, USA
[2]Department of Radiological Sciences, University of California, Los Angeles, CA, USA
[3]Department of Pathology and Laboratory Medicine, University of California, Los Angeles, CA, USA

Address correspondence to: Dr Percy Lee, MD
E-mail: *Percylee@mednet.ucla.edu*

The authors Shaverdian and Yang contributed equally to this work.

Objective: To evaluate the feasibility of on-board diffusion-weighted imaging (DWI) with an integrated low-field MRI radiotherapy system to assess responses to neoadjuvant chemoradiation (NAC) in rectal cancer.
Methods: A spin echo-based planar imaging diffusion sequence on a 0.35-T MRI radiotherapy system was acquired over the course of NAC. The apparent diffusion coefficients (ADCs) from the tumour regions of interest (ROIs) were calculated. A functional diffusion map (fDM) was created showing a pixelwise ADC analysis of the ROI over the course of treatment. Surgical pathology was correlated with ADC data.
Results: Consecutive patients treated on a 0.35-T MRI radiotherapy system were evaluated. Patient A had the worst pathological response to NAC with a tumour regression score of 1 and was the only patient with a negative slope in the change of ADC values over the entire course of NAC, and during both the first and second half of NAC. The fDM from the first half of NAC for Patient A showed discrete dark areas in the tumour ROI, reflecting subregions with decreasing ADC values during NAC. Patient C had the most favourable pathological response to NAC with a Grade 3 response and was the only patient who had an increase in the slope in the change of ADC values from the first to the second half of NAC.
Conclusion: DWI using a low-field MRI radiotherapy system for evaluating the responses to NAC is feasible.
Advances in knowledge: ADC values obtained using a 0.35-T MRI radiotherapy system over the course of NAC for rectal cancer correlate with pathological responses.

INTRODUCTION

Neoadjuvant chemoradiation (NAC) followed by total mesorectal excision is the standard treatment for locally advanced rectal cancer. Responses to chemoradiation vary, but pathological complete response (pCR) rates at the time of surgery range from 10% to 27%.[1–5] There is a growing interest in organ-conserving strategies in rectal cancer to spare patients who have obtained a pCR as predicting these patients up front could spare them from the morbidity of surgery.[6,7] Diffusion-weighted imaging (DWI) is a non-invasive modality that can assess the tissue microenvironment during cancer therapy. The apparent diffusion coefficient (ADC) is calculated from DWI, with low ADC values corresponding to more restricted diffusion, and increases in the ADC post-treatment reflecting the decrease in tumour cellularity as a result of cancer cell death.[8] In the setting of rectal cancer, higher post-NAC ADC values have been found to predict a pCR with diagnostic MR systems.[9–12]

Real-time MRI-guided radiotherapy systems are now available and can potentially allow for the early, longitudinal and seamless assessment of a tumour response to treatment with DWI. Specifically, an integrated 0.35-T MRI radiotherapy system (MRIdian System™, ViewRay™; Cleveland, OH) allows for MRI during each radiation therapy fraction, and the feasibility of performing DWI on this platform has been recently shown.[13] Although DWI has been previously studied in the context of cancer therapy using diagnostic MR systems, the clinical utility of

DWI using an integrated low-field MRI system and its correlation with post-treatment pathological changes is currently unknown.

We report our preliminary experience using this integrated low-field MRI radiotherapy system for the real-time DWI evaluation of treatment responses to NAC in the setting of rectal cancer. We sought to determine whether on-treatment low-field MR DWI data correlated with pathological responses to therapy. Furthermore, we assessed whether a functional diffusion map (fDM) of the gross tumour during MRI-guided radiotherapy would reveal responsive *vs* treatment-resistant subregions.

METHODS AND MATERIALS

Patients and treatment

Three consecutive patients treated on an integrated 0.35-T MRI radiotherapy system as part of a prospective diffusion-weighted (DW) MR imaging protocol were evaluated. The study was approved by our institutional review board. All patients had histologically proven rectal adenocarcinoma and had received NAC with intensity-modulated radiation therapy. Importantly, all patients were staged as having a T4 primary rectal adenocarcinoma. Patients received between 50.4 Gy and 54 Gy to the primary tumour in 1.8-Gy fractions (28–30 daily fractions). Treatment duration ranged from 5.5 to 6 weeks. Radiation was concurrent with oral capecitabine at a dose of 825 mg m^{-2}. Patients underwent post-NAC fludeoxyglucose (FDG)-positron emission tomography (PET) 5.5 weeks after NAC. FDG-PET was performed on a Simens multidetector PET CT scanner using an FDG dose of 0.14 mCi kg^{-1} (Siemens™; Munich, Germany). Surgical resection was scheduled 9–13 weeks after completion of NAC. Pathological responses to NAC were evaluated by a single pathologist who was blinded to all imaging and clinical data. The Dworak criteria were used for pathological response assessment as follows: Grade 0, no regression; Grade 1, minor regression; Grade 2, moderate regression, 26–50% reduction of tumour mass; Grade 3, good regression, >50% reduction of tumour mass; and Grade 4, a pathologic complete response with total regression.[14]

Diffusion-weighted MRI and apparent diffusion coefficient analysis

A previously described spin echo-based echoplanar imaging (EPI) diffusion sequence on the 0.35-T MRI radiotherapy system was used.[13] Imaging was performed immediately after treatment while the patient was still immobilized in the treatment position on the treatment couch. Diffusion images were acquired longitudinally during the course of NAC every 3–7 days depending on patient preference and schedule. For each imaging session, 10 slices were acquired centred at the isocentre and interleaved with the different *b*-values covering the gross tumour volume (GTV). The pulse sequence parameters included: flip angle = 90°, echo time = 160 ms, repetition time = 2600 ms, slice thickness = 6 mm, EPI factor = 128, field of view = 350 × 350 mm^2, *b*-values = 0, 100, 200, 300, 400 and 500 s mm^{-2}, 5 averages and a total scan time of 70 s for all 10 slices. The diffusion images were processed to obtain the ADC maps for each slice using standard monoexponential fitting for each pixel. Excluding low *b*-values or using biexponential fitting may separate out perfusion from ADC. To study the longitudinal relative change of ADC, we are including all *b*-values in our fitting. A region of interest (ROI) was prospectively drawn at the level of the isocentre by the treating radiation oncologist based on the GTV prior to any data acquisition. Our present DWI sequence is a standard DWI sequence which is based on EPI readout. EPI is sensitive to any machine imperfection, which leads to spatial distortion. Taking this into consideration, the radiation oncologist was instructed to draw a smaller ROI within the GTV for the longitudinal ADC analysis to avoid including normal tissues. ADC values from the tumour ROI for each patient were obtained and plotted against the fraction number. A linear trendline was fitted to the ADC values for the entire course of NAC and the slope and R^2 values were calculated. In addition, separate linear trendlines were created for the first half and second half of NAC, to determine the change in the ADC trend between the first and second portion of NAC. Specifically, the first portion of NAC was defined as Fractions 4, 9, 11 and 16 for Patient A, Fractions 4, 6, 11, 16 for Patient B and Fractions 7 and 14 for Patient C. In addition, the primary tumour was contoured on each fraction for which DWI was acquired to measure the primary tumour volume.

A pixelwise longitudinal ADC analysis based on the DWI data was conducted for each patient for the entire course of NAC and for the first half of NAC. The DW images were co-registered using commercial software (MIM Software Inc., Cleveland, OH) and a longitudinal ADC curve was constructed for each voxel within the image. A linear regression of the longitudinal ADC curves for each pixel was performed. And an fDM was generated, where the value of each pixel was the slope of its corresponding linear regression with unit of square millimetre per second × fraction. In each fDM, darker areas represent regions with a negative slope in the change of ADC values throughout NAC.

RESULTS

Patient clinical characteristics

Patient A's pre-treatment FDG-PET showed intense FDG activity involving the inferior two-thirds of the rectum with a maximum standardized uptake value (SUV_{max}) of 7.3. FDG-PET completed 5.5 weeks post-NAC showed residual abnormal FDG activity with an SUV_{max} of 3.7. Surgical resection was performed 13.2 weeks after the completion of NAC. Surgical pathology showed minor evidence of tumour regression with extensive residual cancer, a Grade 1 response (Figure 1).

Patient B's pre-treatment FDG-PET showed a rectal mass with intense FDG activity extending from the anorectal junction to the mid-rectum with an SUV_{max} of 12.9. FDG-PET completed 5.5 weeks post-NAC showed decrease, but residual FDG activity with an SUV_{max} of 4.6. Surgical resection was performed 8.28 weeks after the completion of NAC. Surgical pathology showed evidence of a partial response, scored as Grade 2 tumour regression (Figure 1).

Patient C's pre-treatment FDG-PET showed a mass starting at the rectosigmoid junction with intense FDG uptake with an

Figure 1. Representative pathological slides from surgical resection after neoadjuvant chemoradiation for Patients A, B and C.

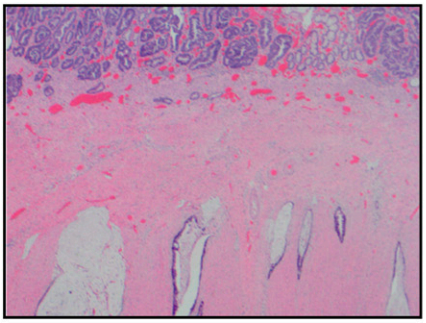

Patient A. Surgical pathology showing little necrosis and extensive residual cancer around mucous glands.

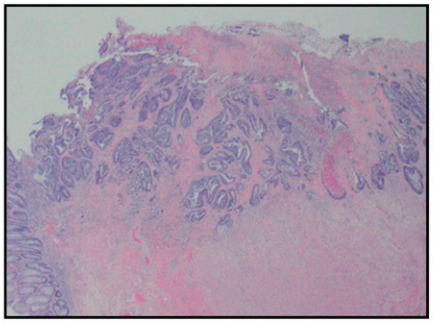

Patient B. Surgical pathology showing necrosis among groups of residual cancer cells.

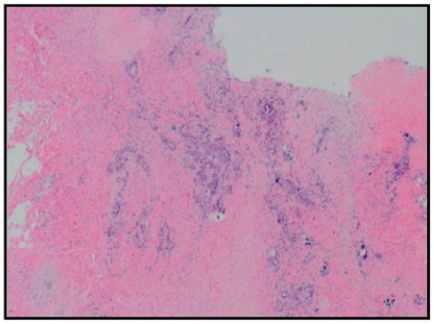

Patient C. Surgical pathology showing abundant necrosis among single and rare groups of cancer cells.

SUV_{max} of 5.7. FDG-PET completed 5.5 weeks post-NAC showed no residual hypermetabolic activity, with an SUV_{max} of 3.1. Surgical resection was performed 10.9 weeks after the completion of NAC. Surgical pathology showed the greatest evidence of tumour regression with only single and groups of residual cancer cells found, scored as a Grade 3 response (Figure 1).

Diffusion-weighted imaging assessment of response to neoadjuvant chemoradiation

Patient A underwent six DWI scans on Fractions 4, 9, 11, 16, 21 and 26 with longitudinal ADC values from the tumour ROI of $1.12\,mm^2\,s^{-1}$, $1.13\,mm^2\,s^{-1}$, $0.97\,mm^2\,s^{-1}$, $1.12\,mm^2\,s^{-1}$, $0.86\,mm^2\,s^{-1}$ and $0.97\,mm^2\,s^{-1}$, respectively (Figure 2a). A best-fit line of the ADC values plotted against time throughout the entire course of NAC had a slope of $-0.0089\,mm^2\,s^{-1}$ fraction ($R^2 = 0.46$). A best-fit line of the ADC values from the first and second portion of NAC had a slope of $-0.075\,mm^2\,s^{-1}$ fraction ($R^2 = 0.7$) and $-0.075\,mm^2\,s^{-1}$ fraction ($R^2 = 0.7$), respectively (Figure 2d).

Patient B underwent seven DWI scans on Fractions 4, 6, 11, 16, 18, 23 and 28 with longitudinal ADC values from the tumour ROI of $0.71\,mm^2\,s^{-1}$, $0.86\,mm^2\,s^{-1}$, $1.18\,mm^2\,s^{-1}$, $1.08\,mm^2\,s^{-1}$, $0.97\,mm^2\,s^{-1}$, $0.89\,mm^2\,s^{-1}$ and $1.09\,mm^2\,s^{-1}$, respectively (Figure 2b). A best-fit line of the ADC values plotted against time throughout the entire course of NAC had a slope of $0.0088\,mm^2\,s^{-1}$ fraction ($R^2 = 0.35$). A best-fit line of the ADC values from the first portion of NAC had a slope of $0.14\,mm^2\,s^{-1}$ fraction ($R^2 = 0.7$), which decreased to $0.06\,mm^2\,s^{-1}$ fraction ($R^2 = 0.7$) for the second portion of NAC (Figure 2d).

Patient C underwent four DWI scans on Fractions 7, 14, 20 and 28 with longitudinal ADC values from the tumour ROI of $0.68\,mm^2\,s^{-1}$, $0.7\,mm^2\,s^{-1}$, $0.84\,mm^2\,s^{-1}$ and $0.95\,mm^2\,s^{-1}$, respectively (Figure 2c). A best-fit line of the ADC values plotted against time throughout the entire course of NAC had a slope of $0.014\,mm^2\,s^{-1}$ fraction ($R^2 = 0.93$). A best-fit line of the ADC values from the first portion of NAC had a slope of $0.02\,mm^2\,s^{-1}$ fraction ($R^2 = 0.66$), which increased to $0.11\,mm^2\,s^{-1}$ fraction ($R^2 = 0.73$) for the second portion of NAC (Figure 2d).

Tumour volume assessment during neoadjuvant chemoradiation

Patient A presented with a primary tumour of 35.2 ml, which measured to be 33.9 ml on Fraction 25, a 3.8% decrease in volume during the course of NAC. Patient B presented with a tumour of 202.4 ml, which was found to be 195.7 ml on Fraction 28, a 3.4% decrease in volume. Patient C presented with a tumour of 110.2 ml, which was found to be 103.9 ml on Fraction 28, reflecting a 5.7% reduction in volume.

Correlation of diffusion-weighted imaging assessment and surgical pathology

Patient A had the worst pathological response to neoadjuvant therapy with a tumour regression score of 1, reflecting only minor evidence of tumour regression. Patient A was the only patient with a negative slope in the change of ADC values over the entire course of NAC, and during both the first and second portion of NAC. Patient A also presented with the highest initial ADC value. In addition, the fDM from the first-half of NAC for Patient A showed discrete dark areas in the tumour ROI, reflecting specific subregions with decreasing ADC values during NAC (Figure 3). Patient C had the most favourable pathological response to NAC with a Grade 3 response, showing >50% regression on surgical pathology. Patient C had the most positive slope in the change of ADC values throughout NAC, and also was the only patient who had an increase in the slope from the first to the second portion of NAC.

DISCUSSION

There is increasing interest in non-operative strategies in rectal cancer management in order to identify patients who achieve a pathological complete response to NAC and therefore allow them to avoid the morbidity of surgical resection.[15,16] However, there is currently no standard method for the early assessment of the efficacy of NAC in rectal cancer. We describe that now with the availability of integrated MRI radiotherapy systems, early, longitudinal and seamless assessments of a tumour response to NAC can be possible with the use of on-board functional MRI.

We show the feasibility of performing longitudinal DWI for evaluating the responses to NAC in the setting of rectal cancer using a low-field MRI radiotherapy system. Our prospective data

Figure 2. (a–c) Mean apparent diffusion coefficient (ADC) values with standard deviations from the region of interest (ROI) throughout neoadjuvant chemoradiation for Patient A, B and C. (d) Mean ADC values from ROI for all three patients with their corresponding linear regression results.

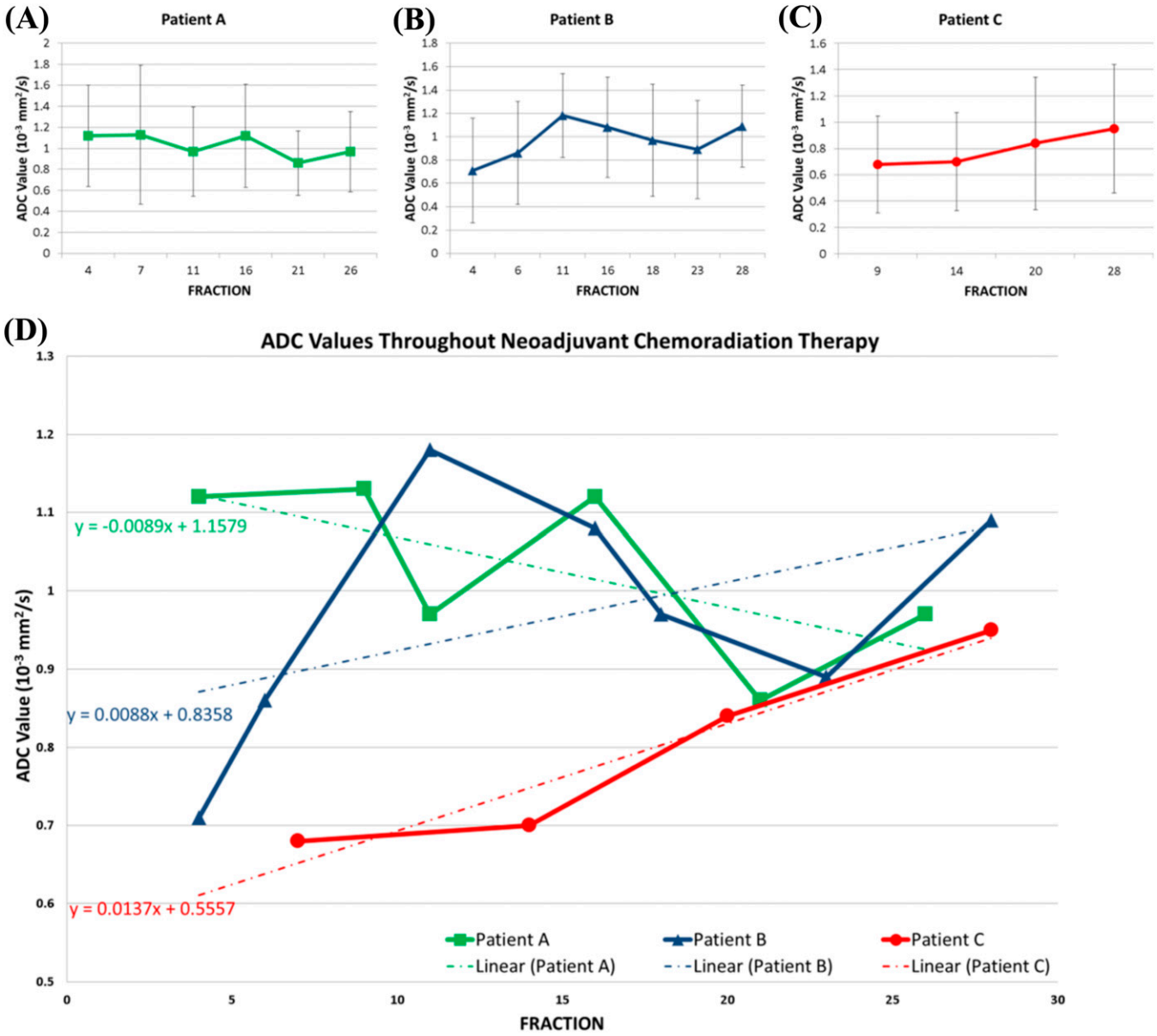

clearly identified the patient with a minimal pathological response to NAC. Specifically, we found the slope of the change in the tumour ADC over the entire course of therapy and over different segments of therapy to be potential early surrogates for treatment response. We also show the feasibility of creating an fDM to show changes in ADC values within tumour subregions during NAC for rectal cancer, allowing for the potential early identification of potential treatment-resistant regions. In addition, we found minimal change to the actual primary tumour volume during the course of NAC, highlighting the value of functional imaging as an early prognostic biomarker.

Previous work has established the clinical utility of functional MRI for response assessment in the setting of rectal cancer using diagnostic MRI systems with 1.5 T or higher field strengths.[9–12] Despite these prior works, our study is novel in several aspects. First, the magnetic strength of the integrated MR radiotherapy system used was 0.35 T to avoid distortion of the radiation dose and thus, we provide important early data on the translatability of these prior findings to a low-field MRI radiotherapy system. Furthermore, given the integration of the MRI and radiotherapy system, longitudinal and seamless DW MR images were acquired on the treatment machine while the patient was still immobilized in the treatment position. This ensures that the DW images are well registered with other images acquired before and after the treatment. Importantly, this integrated approach allows for the creation of an fDM of the tumour, which identifies

Figure 3. Pixelwise longitudinal apparent diffusion coefficient (ADC) analysis showing longitudinal ADC trend of the region of interest (ROI) and differential in ADC value changes within subregions of the ROI. The greyscale represents the slope of the ADC change throughout neoadjuvant chemoradiation (NAC) with units of square millimetre per second fraction. Darker regions represent a negative slope of ADC change throughout NAC, reflecting a decrease in ADC. Brighter regions show a positive slope in ADC value changes, reflecting an increasing ADC. Three images are shown for each patient: (a) shows the high-resolution pre-treatment MRI scan with the primary tumour contoured in white, (b) shows the functional diffusion map (fDM) for the first portion of NAC with the tumour ROI contoured in white and (c) shows the fDM for the entire course of NAC with the tumour ROI contoured in white. Arrows point to discrete areas of darkness within the tumour ROI for Patient A during the first portion of NAC, highlighting a potential treatment-resistant subregion.

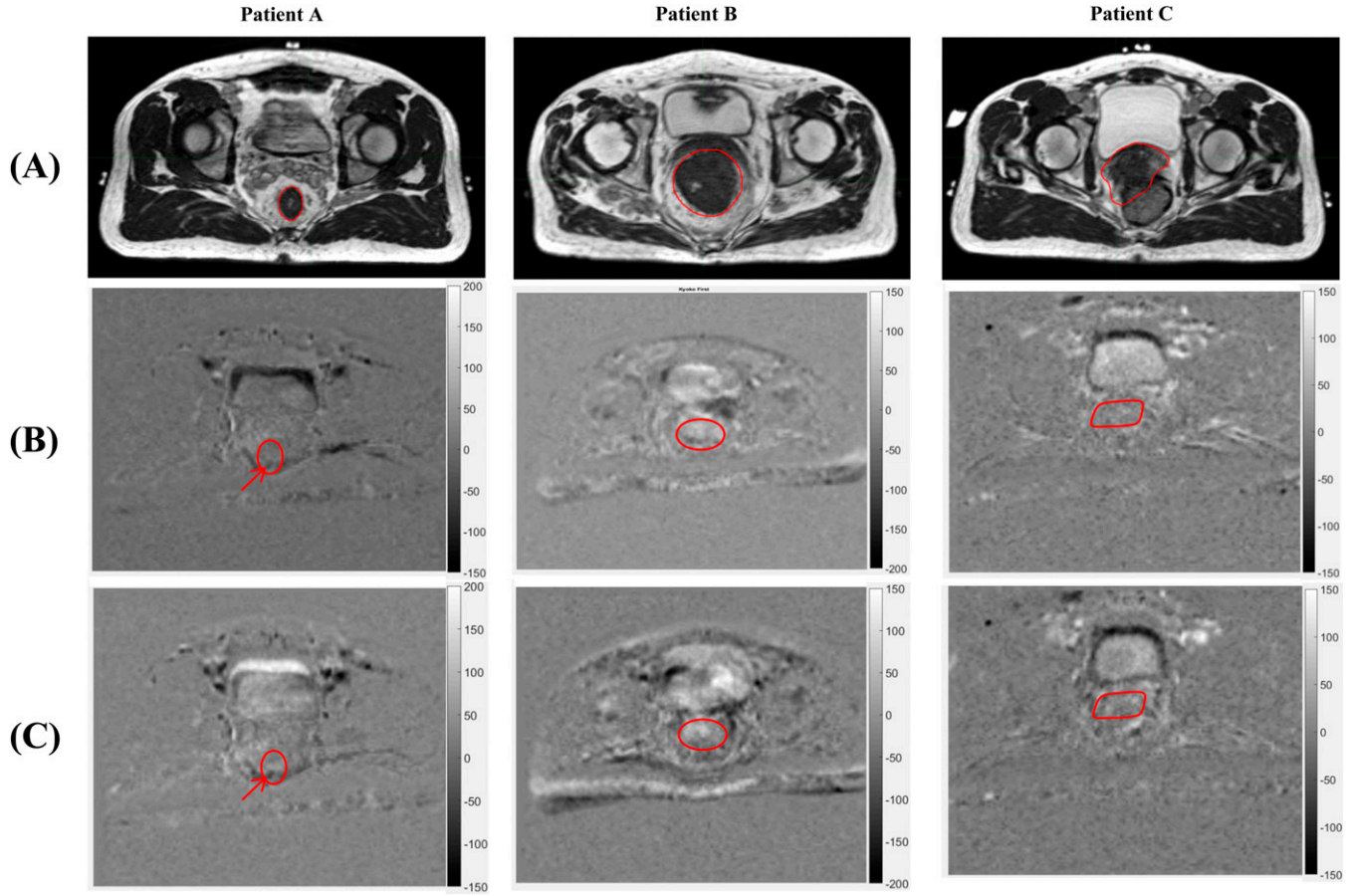

pixelwise trends in ADC changes over the course of treatment, allowing for the identification of potential treatment-resistant regions. More extensive studies evaluating the utility of fDMs have been completed in the setting of malignant gliomas, where it has been found that the volume of tumour with increasing diffusion seen on an fDM during definitive chemo-radiation is an independent prognostic factor for survival.[17] These previous studies have highlighted the potential utility of DWI data to guide personalized treatment intensification strategies with novel boost plans that target resistant regions based off the fDM.[18,19]

This study, although clearly limited in patient size, shares an important preliminary experience of the use of functional MRI with an integrated low-field MRI radiotherapy system in the setting of rectal cancer. Other limitations include baseline differences in patient age and sex, and differences in the lengths of time between the end of NAC and surgery. Despite these limitations, this preliminary experience shows the great potential of MRI-guided radiotherapy that warrants further research.

In conclusion, prior work has shown DWI to provide an early and accurate assessment of the efficacy of chemoradiation. MRI radiotherapy systems allow for the integration of this powerful modality into radiation therapy. Further use and investigation is necessary, especially in the setting of rectal cancer, where novel imaging techniques can better select patients suitable for non-operative management, and where pathological correlation can allow for greater investigation of the integration of functional MRI with radiation therapy.

CONFLICTS OF INTEREST

Dr Michael Steinberg serves on the scientific advisory board of ViewRay. Dr Daniel Low serves as a consultant for ViewRay. Dr Percy Lee has received a speaking honorarium from ViewRay. Dr Minsong Cao and Dr James Lamb have performed consulting work for ViewRay.

REFERENCES

1. Das P, Skibber JM, Rodriguez-Bigas MA, Feig BW, Chang GJ, Wolff RA, et al. Predictors of tumor response and downstaging in patients who receive preoperative chemo radiation for rectal cancer. *Cancer* 2007; **109**: 1750–5. doi: https://doi.org/10.1002/cncr.22625
2. Sauer R, Becker H, Hohenberger W. Preoperative *versus* postoperative chemoradiotherapy for rectal cancer. *N Engl J Med* 2004; **351**: 1731–40. doi: https://doi.org/10.1056/NEJMoa040694
3. Rodel C, Martus P, Papadoupolos T. Prognostic significant for tumor regression after preopative chemoradiotherapy for rectal cancer. *J Clin Oncol* 2005; **23**: 8688–96. doi: https://doi.org/10.1200/JCO.2005.02.1329
4. Park IJ, You YN, Agarwal A, Skibber JM, Rodriguez-Bigas MA, Eng C, et al. Neoadjuvant treatment response as an early response indicator for patients with rectal cancer. *J Clin Oncol* 2012; **30**: 1770–6. doi: https://doi.org/10.1200/JCO.2011.39.7901
5. Maas M, Nelemans PJ, Valentini V, Das P, Rödel C, Kuo LJ, et al. Long-term outcome in patients with a pathological compete response after chemoradiation for rectal cancer: a pooled analysis of individual patient data. *Lancet Oncol* 2010; **11**: 835–44. doi: https://doi.org/10.1016/S1470-2045(10)70172-8
6. Garcia-Aguilar J, Renfro LA, Chow OS, Shi Q, Carrero XW, Lynn PB, et al. Organ preservation for clinical T2N0 distal rectal cancer using neoadjuvant chemoradiotherapy and local excision (ACOSOG Z6041): results of an open-label, single-arm, multiinstitutional, Phase 2 trial. *Lancet Oncol* 2015; **16**: 1537–46. doi: https://doi.org/10.1016/S1470-2045(15)00215-6
7. Yang TJ, Goodman KA. Predicting complete response: is there a role for non-operative management of rectal cancer? *J Gastrointest Oncol* 2015; **6**: 241–6. doi: https://doi.org/10.3978/j.issn.2078-6891.2014.110
8. Malayeri AA, El Khouli RH, Zaheer A, Jacobs MA, Corona-Villalobos CP, Kamel IR, et al. Principles and applications of diffusion-weighted imaging in cancer detection, staging and treatment follow-up. *Radiographics* 2011; **31**: 1773–91. doi: https://doi.org/10.1148/rg.316115515
9. Cai G, Xu Y, Zhu J, Gu WL, Zhang S, Ma XJ, et al. Diffusion-weighted magnetic resonance imaging for predicting the response of rectal cancer to neoadjuvant concurrent chemoradiation. *World J Gastroenterol* 2013; **19**: 5520–7. doi: https://doi.org/10.3748/wjg.v19.i33.5520
10. Lambregts DM, Rao SX, Sassen S, Martens MH, Heijnen LA, Buijsen J, et al. MRI and Diffusion-weighted MRI volumetry for identification of complete tumor responders after preoperative chemoradiotherapy in patients with rectal cancer. *Ann Surg* 2015; **262**: 1034–9. doi: https://doi.org/10.1097/SLA.0000000000000909
11. Joye I, Deroose CM, Vandecaveye V, Haustermans K. The role of diffusion-weighted MRI and PET/CT in the prediction of pathologic complete response after radiochemotherapy for rectal cancer: a systematic review. *Radiother Oncol* 2014; **113**: 158–65. doi: https://doi.org/10.1016/j.radonc.2014.11.026
12. Xie H, Sun T, Chen M, Wang H, Zhou X, Zhang Y, et al. Effectiveness of the apparent diffusion coefficient for predicting the response to chemoradiation therapy in locally advanced rectal cancer. *Medicine (Baltimore)* 2015; **94**: e517. doi: https://doi.org/10.1097/md.0000000000000517
13. Yang Y, Cao M, Sheng K, Gao Y, Chen A, Kamrava M, et al. Longitudinal diffusion MRI for treatment response assessment: preliminary experience using an MRI-guided tri-cobalt 60 radiotherapy system. *Med Phys* 2016; **43**: 1369–73. doi: https://doi.org/10.1118/1.4942381
14. Dworak O, Keilholz L, Hoffman A. Pathological features of rectal cancer after preoperative radiochemotherapy. *Int J Colorectal Dis* 1997; **12**: 19–23. doi: https://doi.org/10.1007/s003840050072
15. Ellis CT, Samuel CA, Stitzenberg KB. National trends in nonoperative management of rectal adenocarcinoma. *J Clin Oncol* 2016; **34**: 1644–51. doi: https://doi.org/10.1200/JCO.2015.64.2066
16. Torok JA, Palta M, Willet CG, Czito BG. Nonoperative management of rectal cancer. *Cancer* 2016; **122**: 34–41. doi: https://doi.org/10.1002/cncr.29735
17. Hamstra DA, Glaban CJ, Meyer CR, Johnson TD, Sundgren PC, Tsien C, et al. Functional diffusion map as an early imaging biomarker for high-grade glioma: correlation with conventional radiologic response and overall survival. *J Clin Oncol* 2008; **26**: 3387–94. doi: https://doi.org/10.1200/JCO.2007.15.2363
18. Galban CJ, Chenevert TL, Meyer CR, Tsien C, Lawrence TS, Hamstra DA, et al. Prospective analysis of parametric MRI biomarkers: identification of early and distinct glioma response patterns not predicted by standard radiographic assessment. *Clin Cancer Res* 2011; **17**: 4751–60. doi: https://doi.org/10.1158/1078-0432.CCR-10-2098
19. Tsien C, Cao Y, Chenevert T. Clinical applications for diffusion MRI in radiotherapy. *Semin Radiat Oncol* 2014; **24**: 218–26. doi: https://doi.org/10.1016/j.semradonc.2014.02.004